Journal of Sound and Vibration (1997) **201**(5), 641–647

STRIP DISTRIBUTED TRANSFER FUNCTION ANALYSIS OF CIRCULAR AND SECTORIAL PLATES

B. Yang and J. Zhou

Department of Mechanical Engineering, University of Southern California, Los Angeles, CA 90089-1453, *U.S.A*

(*Received* 9 *October* 1995, *and in final form* 26 *July* 1996)

1. INTRODUCTION

Various solution methods have been developed for static and dynamic problems of plates, among which are the finite element method, finite difference method, finite strip method, Fourier-Bessel series technique, Rayleigh-Ritz method, Galerkin method, and assumed modes method [1–7]. Although the finite element method, as a powerful numerical tool, has met with great success in engineering applications, analytical solutions are always desirable, for the latter are more accurate and provide physical insight into the problem. Recently, a semi-analytical method, called the Strip Distributed Transfer Function Method (SDTFM), was developed for modeling and analysis of two-dimensional elastic continua composed of rectangular subregions [8, 9].

In this letter, the concept of SDTFM is extended to plates that are confined in circular or sectorial regions. The major thrust of SDTFM is to combine the high accuracy of analytical solutions, and the flexibility of the finite element method in modeling complex geometry and arbitrary boundary conditions. Furthermore, the method delivers closed-form solutions without using truncated series of particular comparison or admissible functions, and therefore is capable of precisely modeling of abrupt changes in system properties and disturbance distributions. The numerical examples reveal many advantages of SDTFM.

2. METHOD

The sectorial plate in Figure 1, in the polar co-ordinate system, is confined in the domain

$$\{(r, \theta, z) \mid R_0 \leqslant r \leqslant R_1, -\theta_0 \leqslant \theta \leqslant \theta_0, -0{\cdot}5h(r) \leqslant z \leqslant 0{\cdot}5h(r)\}, \tag{1}$$

where $2\theta_0$ is the angle subtended by the sector, and $h(r)$ is the thickness of the plate. Here h is allowed to vary along the radial direction, but is constant in the circumferential direction. For a circular plate, $2\theta_0 = 2\pi$. In analysis of a circular/sectorial plate, the proposed SDTFM takes three major steps: (a) interpolation of the plate deflection in terms of nodal line displacements; (b) derivation of the governing equations of the nodal line displacements; and (c) determination of the nodal line displacements and plate responses by strip distributed transfer functions. These steps are briefly discussed as follows.

The plate is divided into NS strips by $NS + 1$ circumferential lines, see Figure 1, where r_j is the radius of the jth line. These lines are called nodal lines and their ends are named nodes. The jth strip, bounded by the jth and $(j + 1)$th nodal lines, is defined by

$$\Omega_j = \{(r, \theta) \mid r_j \leqslant r \leqslant r_{j+1}, -\theta_0 \leqslant \theta \leqslant \theta_0\}, \tag{2}$$

0022–460X/97/150641 + 07 $25.00/0/sv960712

whose width $b_j = r_{j+1} - r_j$. To increase the accuracy of displacement interpolation, internal nodal lines can be introduced within a strip. The transverse displacement of the jth strip of the plate is interpolated in the radial co-ordinate

$$w(r, \theta, t) = [\mathbf{N}_w(r)]\{\mathbf{W}_j(\theta, t)\}, \qquad (r, \theta) \in \Omega_j, \tag{3}$$

where $[\mathbf{N}_w(r)]$ is the shape function matrix. The vector $\{\mathbf{W}_j(\theta, t)\}$ contains the unknown displacement parameters on the nodal lines of the jth strip. For instance, in a cubic interpolation without internal nodal line displacements,

$$[\mathbf{N}_w] = [1 - 3\xi^2 + 2\xi^3 \quad b_i(\xi - 2\xi^2 + \xi^3) \quad 3\xi^2 - 2\xi^3 \quad b_i(-\xi^2 + \xi^3)], \tag{4}$$

$$\{\mathbf{W}_j(\theta, t)\} = \{w_j(\theta, t) \quad \beta_j(\theta, t) \quad w_{j+1}(\theta, t) \quad \beta_{j+1}(\theta, t)\}^{\mathrm{T}}, \tag{5}$$

where $\xi = (r - r_i)/b_i$, and

$$w_j(\theta, t) = w(r_j \theta, t), \qquad \beta_j(\theta, t) = (\partial/\partial r)\, w(r, \theta, t)|_{r = r_j} \tag{6}$$

are the displacement and rotation of the plate on the jth nodal line, respectively.

Assume that the plate is made of linear elastic material under small deformation. The Hamilton principle for the plate is

$$\int_{t_1}^{t_2} \delta \left\{ \int_{-\theta_0}^{\theta_0} \int_{-R_0}^{R_1} \left(\tfrac{1}{2}\{\kappa\}^{\mathrm{T}}[\mathbf{D}]\{\boldsymbol{\kappa}\} - \tfrac{1}{2}\rho \dot{w}^2\right) r \,\mathrm{d}r\,\mathrm{d}\theta \right\} \mathrm{d}t$$

$$- \int_{t_1}^{t_2} \left\{ \int_{-\theta_0}^{\theta_0} \int_{-R_0}^{R_1} q \delta w r \,\mathrm{d}r\,\mathrm{d}\theta + \int_{R_0}^{R_1} \left(\bar{Q}_\theta\, \delta w + \bar{M}_\theta \delta \frac{\partial w}{r \partial \theta} \right.\right.$$

$$\left.\left. + \bar{M}_{r\theta} \delta \frac{\partial w}{\partial r} \right)\Bigg|_{\theta = \pm\theta_0} \mathrm{d}r \right\} \mathrm{d}t = 0, \tag{7}$$

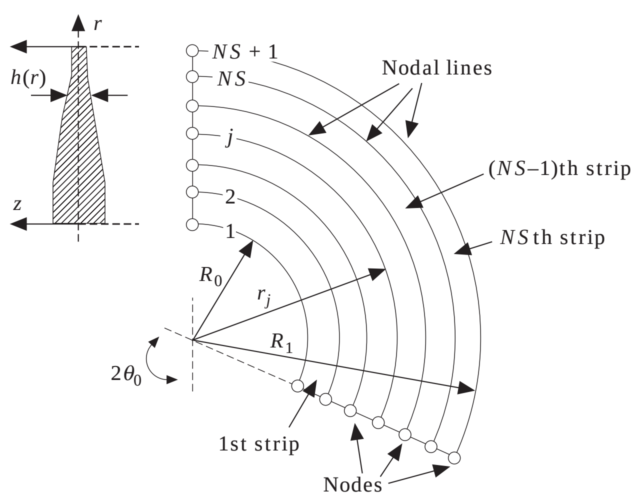

Figure 1. A sectorial plate divided into strips.

where $\{\boldsymbol{\kappa}\}$ is the curvature vector of the form [4]

$$\{\boldsymbol{\kappa}\} = \left\{ -\frac{\partial^2 w}{\partial r^2} - \frac{\partial^2 w}{r^2\,\partial\theta^2} - \frac{\partial w}{r\partial r} - \frac{2}{r}\frac{\partial^2 w}{\partial r\,\partial\theta} + \frac{2}{r^2}\frac{\partial w}{\partial\theta} \right\}^{\mathrm{T}}, \tag{8}$$

$[\mathbf{D}]$ is the bending stiffness matrix, ρ is the density per unit area, q is the transverse external force applied on the neutral surface of the plate, $\bar{Q}_\theta$, $\bar{M}_\theta$ and $\bar{M}_{r\theta}$ are the shear force, bending moment and torsional moment on the boundaries $\theta = \pm\theta_0$, respectively, and δ denotes variation of the displacement function.

Substituting equation (3) into equation (7) and conducting the variation, one obtains the partial differential equation governing the nodal line displacements [8, 9]:

$$\left([\mathbf{M}]\frac{\partial^2}{\partial t^2} + \sum_{i=0}^{4}[\mathbf{K}_i]\frac{\partial^i}{\partial\theta^i}\right)\{\boldsymbol{\Phi}(\theta, t)\} = \{\mathbf{Q}(\theta, t)\}, \qquad -\theta_0 \leqslant \theta \leqslant \theta_0, \tag{9}$$

where the constant matrices $[\mathbf{M}]$ and $[\mathbf{K}_i]$ describe the inertia and stiffness of the plate, $\{\mathbf{Q}(\theta, t)\}$ is the nodal line force vector, and $\{\boldsymbol{\Phi}(\theta, t)\}$ is the global nodal line displacement vector consisting of all independent nodal line displacements of the NS strips. Without loss of generality, assume zeros initial conditions for the plate. Taking the Laplace transform of equation (9) with respect to t, and casting the resulting equation in a first-order, spatial state-space form [8, 9] yields

$$(\mathrm{d}/\mathrm{d}\theta)\{\eta(\theta, s)\} = [\mathbf{F}(s)]\{\eta(\theta, s)\} + \{\mathbf{f}(\theta, s)\}, \qquad -\theta_0 \leqslant \theta \leqslant \theta_0, \tag{10}$$

where s is the Laplace transform parameter; the state-space matrix $[\mathbf{F}(s)]$ and the load vector $\{\mathbf{f}(\theta, s)\}$ are derived from the inertia and stiffness matrices and the nodal line force vector in equation (9), respectively, and the state-space vector

$$\{\eta(\theta, s)\} = \{\hat{\Phi}^{\mathrm{T}}(\theta, s)(\mathrm{d}/\mathrm{d}\theta)\hat{\Phi}^{\mathrm{T}}(\theta, s)\,(\mathrm{d}^2/\mathrm{d}\theta^2)\hat{\Phi}^{\mathrm{T}}(\theta, s)(\mathrm{d}^3/\mathrm{d}\theta^3)\hat{\Phi}^{\mathrm{T}}(\theta, s)\}^{\mathrm{T}}, \tag{11}$$

with $\hat{\Phi}(\theta, s)$ being the Laplace transform of $\{\boldsymbol{\Phi}(\theta, t)\}$. The boundary conditions of the nodal line displacements are specified at the nodes of the nodal lines. Following the above derivation, these boundary conditions are cast in the form

$$[\mathbf{M}_b(s)]\{\eta(-\theta_0, s)\} + [\mathbf{N}_b(s)]\{\eta(\theta_0, s)\} = \{\boldsymbol{\gamma}(s)\}, \tag{12}$$

where the boundary matrices $[\mathbf{M}_b(s)]$ and $[\mathbf{N}_b(s)]$ are constant matrices, and the vector $\{\boldsymbol{\gamma}(s)\}$ describes the given boundary disturbances [8, 9].

The solution of the state-space equations (10) and (12) is in exact and closed form [10]

$$\{\eta(\theta, s)\} = \int_{-\theta_0}^{\theta_0}[\mathbf{G}(\theta, \zeta, s)]\{\mathbf{f}(\zeta, s,)\}\,\mathrm{d}\zeta + [\mathbf{H}(\theta, s)]\{\boldsymbol{\gamma}(s)\}, \tag{13}$$

where

$$[\mathbf{G}(\theta, \xi, s)] = \begin{cases} [\mathbf{H}(\theta, s)][\mathbf{M}_b(s)]\,\mathrm{e}^{-[\mathbf{F}(s)](\theta_0+\zeta)}, & \xi \leqslant \theta \\ -[\mathbf{H}(\theta, s)][\mathbf{N}_b(s)]\,\mathrm{e}^{[\mathbf{F}(s)](\theta_0-\zeta)}, & \xi \geqslant \theta, \end{cases} \tag{14a}$$

$$[\mathbf{H}(\theta, s)] = \mathrm{e}^{[\mathbf{F}(s)]\theta}([\mathbf{M}_b(s)]\,\mathrm{e}^{-\theta_0[\mathbf{F}(s)]} + [\mathbf{N}_b(s)]\,\mathrm{e}^{\theta_0[\mathbf{F}(s)]})^{-1}. \tag{14b}$$

The matrices $[\mathbf{G}(\theta, \zeta, s)]$ and $[\mathbf{H}(\theta, s)]$ are termed the strip distributed transfer functions of the circular/sectorial plate.

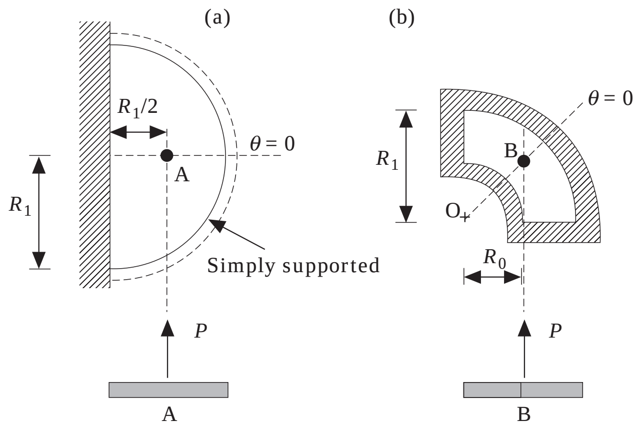

Figure 2. Sectorial plates: (a) System I—a clamped-simply supported semi-circular plate; and (b) System II—a clamped quarter annular sector, $|OB| = (R_0 + R_1)/2$.

The distributed transfer function formulation is convenient in predicting the response of the plate. The static response of the plate is obtained by equation (13) with $s = 0$; the dynamic response to a harmonic excitation of frequency ω is found by setting $s = J\omega$, $J = \sqrt{-1}$, in equation (13). In free vibration analysis, the characteristic equation of the plate is

$$\det\left([\mathbf{M}_b(s)]\, e^{-\theta_0[\mathbf{F}(s)]} + [\mathbf{N}_b(s)]\, e^{\theta_0[\mathbf{F}(s)]}\right) = 0 \tag{15}$$

whose roots are the eigenvalues of the plate.

3. NUMERICAL RESULTS

The SDTFM is illustrated on two plate systems shown in Figure 2: (a) System I—a clamped-simply supported semi-circular plate subject to a transverse load P at point A ($\theta = 0$, $r = R_1/2$); and (b) System II—a clamped quarter annular sector ($2\theta_0 = \pi/2$) subject to a transverse load P at point B ($\theta = 0$, $r = (R_0 + R_1)/2$). Both plates are isotropic, and of uniform thickness. The plate parameters are chosen as $R_0 = 20$, $R_1 = 100$, $h = 1$, $E = 10^6$, $\upsilon = 0{\cdot}3$, where h is plate thickness, E is Young's module, and υ is Poisson's ratio.

Static deflections and natural frequencies are calculated by SDTFM with strips of equal width and the cubic strip displacement interpolation given in equations (4) and (5), and by the finite element method (FEM). Figure 3 shows the static deflection of System I (the semi-circular plate) along the circumferential line $r = R_1/2$. Figure 4 shows the static deflection of System II (annular sector) along the circumferential line $r = (R_0 + R_1)/2$. Since exact solutions are not available, the predictions by FEM with dense meshes (24×64 and 32×32 elements for Systems I and II, respectively) serve as reference solutions. With just fourth strips, the results obtained by SDTFM are in good agreement with the reference solutions. Even two strips are accurate enough.

In free vibration analysis, the first 10 natural frequencies are computed, and listed in Tables 1 and 2. The accuracy of SDTFM is surprisingly high. For System I (Table 1), the fourth strip SDTFM prediction has a maximum deviation of 1·2% from the reference solution, which is obtained by FEM with a 16×64 mesh (1,024 elements). However, FEM with the less dense 4×16, 6×24 and 8×32 meshes leads to much larger deviations of

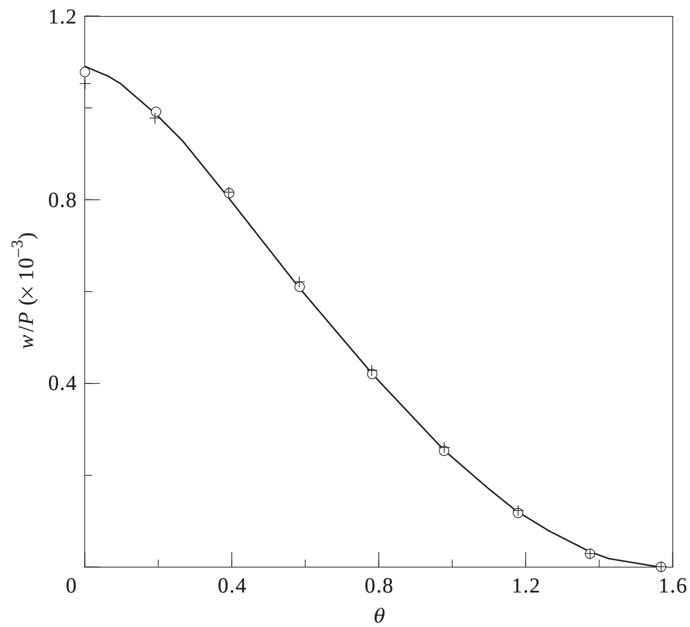

Figure 3. Static deflection of the semi-circular plate (System I) at $r = R_1/2$: ——, FEM of 24×64 elements; + + +, SDTFM of 2 strips; ○ ○ ○, SDTFM of 4 strips.

31·4%, 19·1% and 9·6%, respectively. Note that 4-strip prediction is more accurate than the reference solution, since the natural frequencies calculated by SDTFM are less than those by FEM. The 6-strip prediction has even higher precision.

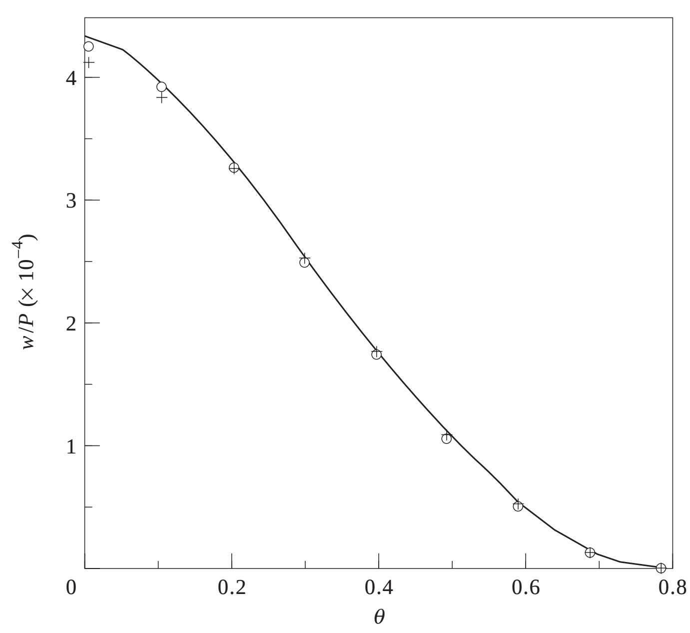

Figure 4. Static deflection of the annular sector (System II) at $r = (R_0 + R_1)/2$: ——, FEM of 32×32 elements; + + +, SDTFM of 2 strips; ○ ○ ○, SDTFM of 4 strips.

Table 1

Natural frequencies of the semi-circular plate, System I

Mode no.	SDTFM 4 strips	SDTFM 6 strips	FEM 4×16 mesh	FEM 6×24 mesh	FEM 8×32 mesh	FEM 16×64 mesh
1	0·5903	0·5901	0·6428	0·6055	0·5986	0·5920
2	0·9522	0·9513	1·0191	1·9818	0·9683	0·9552
3	1·4116	1·4105	1·5383	1·4701	1·4442	1·4184
4	1·7790	1·7723	2·1606	1·9520	1·8721	1·7951
5	1·9559	1·9538	2·1749	2·0587	2·0133	1·9676
6	2·4290	2·4127	2·9309	2·6801	2·5619	2·4460
7	2·4290	2·4127	2·9309	2·6801	2·5619	2·4460
8	3·1865	3·1681	3·8048	3·5420	3·3932	3·2198
9	3·2748	3·2685	3·9368	3·5623	3·4273	3·3069
10	3·6166	3·5642	4·8091	4·3585	4·0094	3·6596

For System II, similar conclusions can be drawn from Table 2. Although Tables 1 and 2 only list the first 10 natural frequencies, further numerical simulation indicates that SDTFM is even more accurate than the FEM in predicting higher-order natural frequencies.

4. CONCLUSIONS

The strip distributed transfer function method for analysis of circular and sectorial plates has been presented. With its semi-analytical form, SDTFM is much more accurate than the finite element method in predicting the static deflection and natural frequencies of circular and sectorial plates. Like the finite element method, SDTFM is versatile in modelling complex geometry and various boundary conditions of plate structures, which is difficult for many existing analytical or semi-analytical methods. While the thin plate theory is used in this study, the proposed method can be easily extended to other plate theories. Moreover, SDTFM can further increase its accuracy by introducing higher-order interpolation models. Additionally, SDTFM is applicable to complex plate structures composed of multiple circular/sectorial subregions [9].

Table 2

Natural frequencies of the annular sector, System II

Mode no.	SDTFM 4 strips	SDTFM 6 strips	FEM 4×4 mesh	FEM 8×8 mesh	FEM 16×16 mesh	FEM 32×64 mesh
1	1·5241	1·5226	1·6162	1·5514	1·5292	1·5227
2	2·6615	2·6586	3·0212	2·7984	2·6937	2·6597
3	3·4804	3·4567	3·8479	3·6232	3·4940	3·4596
4	4·1556	4·1469	3·8893	4·5996	4·2651	4·1515
5	5·0325	5·0121	4·8714	5·3623	5·1012	5·0179
6	5·9435	5·9219	5·6212	6·3347	6·2171	5·9331
7	6·4031	6·3094	7·0808	6·8958	6·4337	6·3089
8	7·1800	7·1410	7·6215	6·9984	7·3720	7·1541
9	8·0295	7·9811	9·0179	7·9760	8·2625	8·0037
10	8·1748	8·0619	12·504	8·8788	8·5985	8·0673

ACKNOWLEDGMENT

This work was partially supported by the US Army Research Office.

REFERENCES

1. S. P. TIMOSHENKO 1940 *Theory of Plates and Shells*. New York: McGraw-Hill.
2. A. W. LEISSA 1981 *Shock and Vibration Digest* **13**, 19–36. Plate vibration research 1976–1980: complicating effects.
3. A. W. LEISSA 1981 *Shock and Vibration Digest* **19**, 11–18. Recent studies in plate vibrations, 1981–1985, part I. classical theory.
4. W. SOEDEL 1993 *Vibration of Shells and Plates*. New York: Marcel Dekker; (second edition).
5. O. C. ZIENKIEWICZ and R. L. TAYLOR 1989 *The Finite Element Method*. New York: McGraw-Hill.
6. L. MEIROVITCH 1967 *Analytical Methods in Vibrations*. London: the Macmillan Company
7. Y. K. CHEUNG 1976 *Finite Strip Method in Structural Analysis*. Oxford, U.K.: Pergamon Press.
8. J. ZHOU and B. YANG 1996 *International Journal for Numerical Methods in Engineering* **39**, 1915–1932. Strip distributed transfer function method for analysis of plates.
9. B. YANG and J. ZHOU 1996 *International Journal of Solid and Structures* **33**, 3983–4005. Semi-analytical solution of 2-D elasticity problems by the strip distributed transfer function method.
10. B. YANG and C. A. TAN 1992 *ASME Journal of Applied Mechanics* **59**, 1009–1014. Transfer functions of one-dimensional distributed parameter systems.